

星形成ゼミ

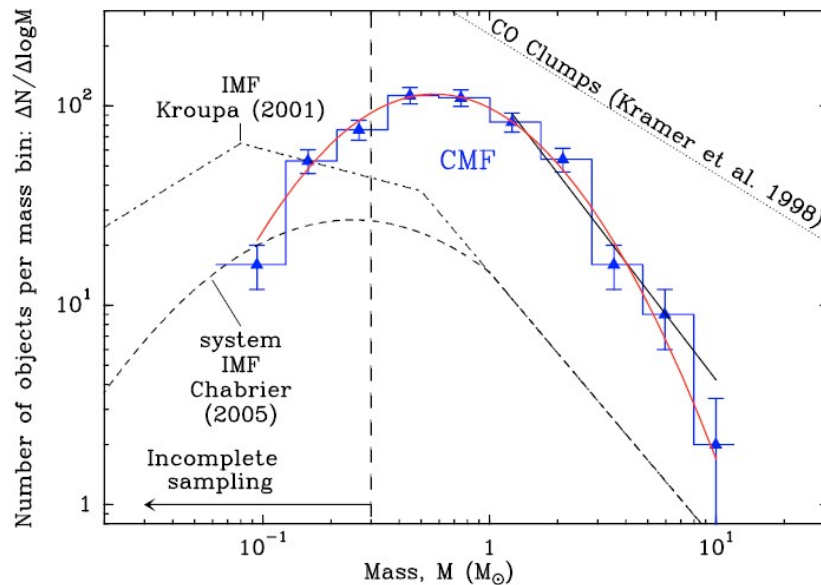
岩崎一成 (国立天文台)

1. Probing the initial conditions of high-mass star formation. III. Fragmentation and triggered star formation
Zhang+
2. **The role of molecular filaments in the origin of the prestellar core mass function and stellar initial mass function**
Andre+
3. The Transition from a Lognormal to a Power-law Column Density Distribution in Molecular Clouds: An Imprint of the Initial Magnetic Field and Turbulence
Auddy+
4. The Concentration and Growth of Solids in Fragmenting Circumstellar Disks
Baehr & Klahr
5. OH maser emission in the THOR survey of the northern Milky Way
Beuther+
6. First detections of H₁₃CO⁺ and HC₁₅N in the disk around HD 97048: Evidence for a cold gas reservoir in the outer disk
Booth+

The role of molecular filaments in the origin of the prestellar core mass function and stellar initial mass function

Ph. André¹, D. Arzoumanian^{2,3,1}, V. Könyves^{4,1}, Y. Shimajiri^{5,1,6}, and P. Palmeirim³

- フィラメント中での星形成 (Andre+ 2010...)
 - 高密度コアの>75%は超臨界のフィラメント中に存在 ($ML > 2cs^2/G \sim 16 M_{\text{sun}}/\text{pc}$)
 - フィラメント形成 → コア形成 → 星形成
- 初期質量関数～コア質量関数 (Motte+1998,...)

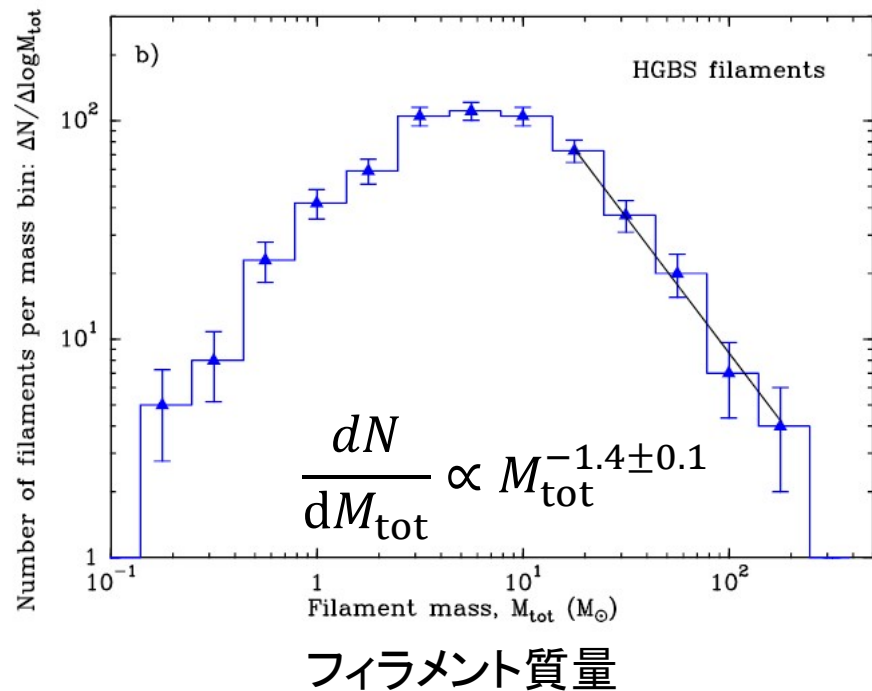
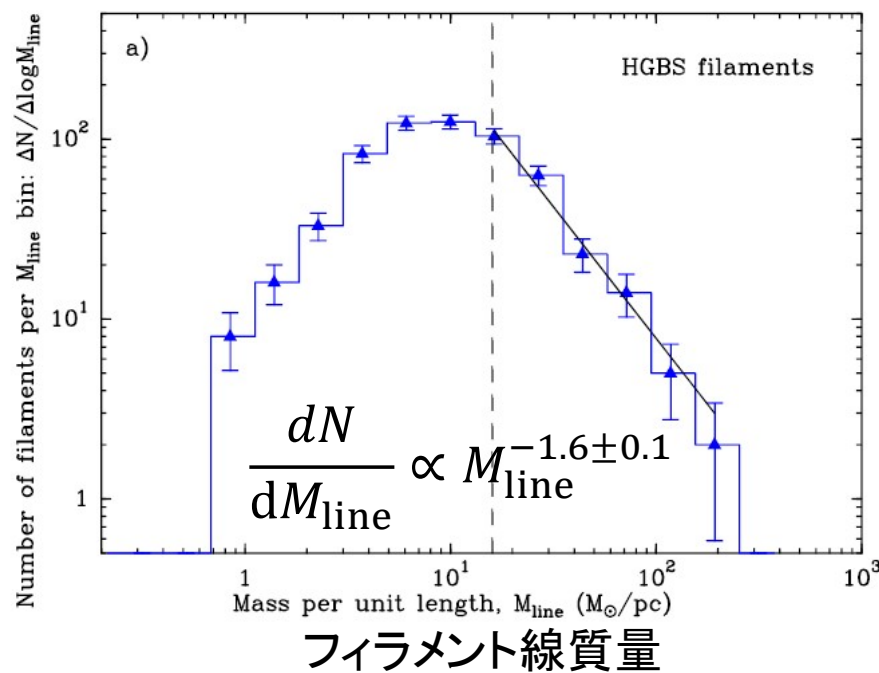


Andre et al. 2010

- フィラメントはどう初期質量関数に関係するか？

フィラメントの質量関数

599本のフィラメント(IC5146, Orion B, Aquila, Musca, Polaris, Pipe, Taurus L1495, Ophiuchus)
Aspect ratio > 3 and column density contrast $\delta\Sigma_{\text{fil}}/\Sigma_{\text{cloud}} > 30\%$



- フィラメントの質量関数の冪はIMFと似ている

Toy model

$$\xi(m) = \int f_{M_{\text{line}}}(m) \times w(M_{\text{line}}) \times g(M_{\text{line}}) \times d\log M_{\text{line}},$$

Mlineのフィラメントに形成されるコアの質量関数

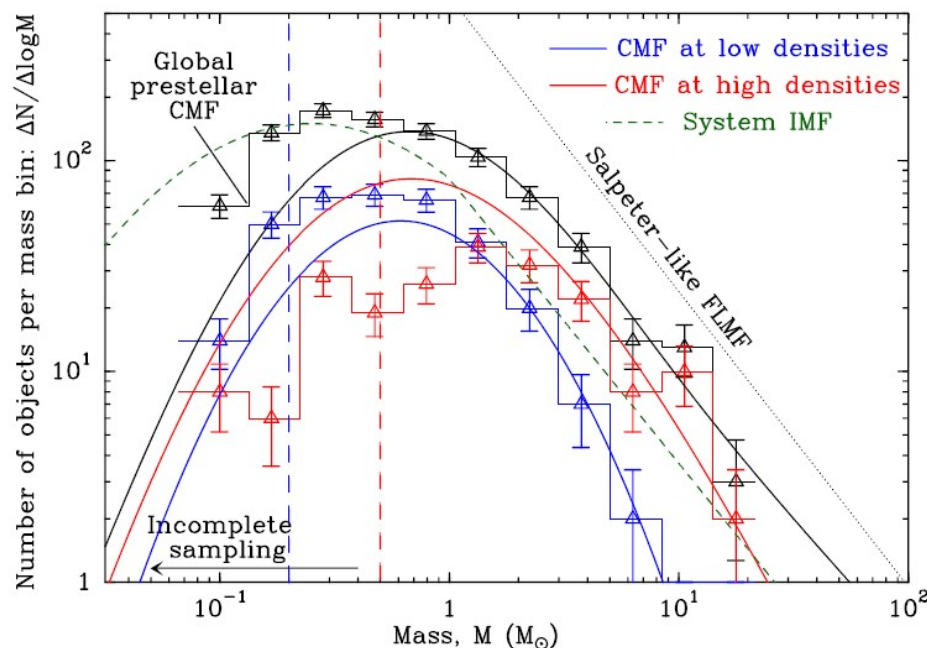
$$dN_{M_{\text{li}}} = \frac{dN_{M_{\text{lin}}}}{d\log m}$$

Bonnor-Ebert massを中心とするlog normal

フィラメントの中でコアになる質量



- $M_{\text{line}} < M_{\text{line}}^{\text{crit.}}$: 0
- $M_{\text{line}} > M_{\text{line}}^{\text{crit.}}$: 15-20% (Konyves+2015)

フィラメント線密度の頻度分布



フィラメント線密度の頻度分布が直接CMFの冪になっているという主張

The Concentration and Growth of Solids in Fragmenting Circumstellar Disks

Hans Baehr¹  and Hubert Klahr 

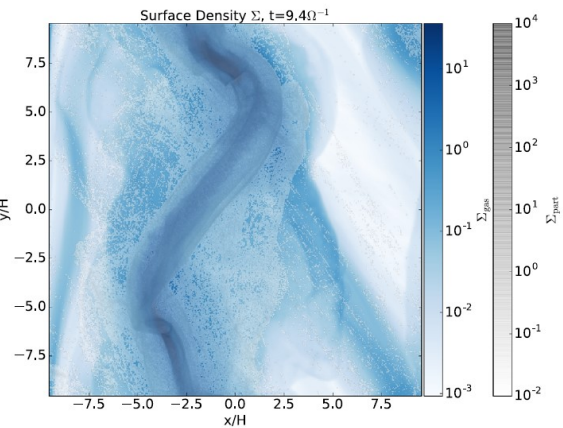
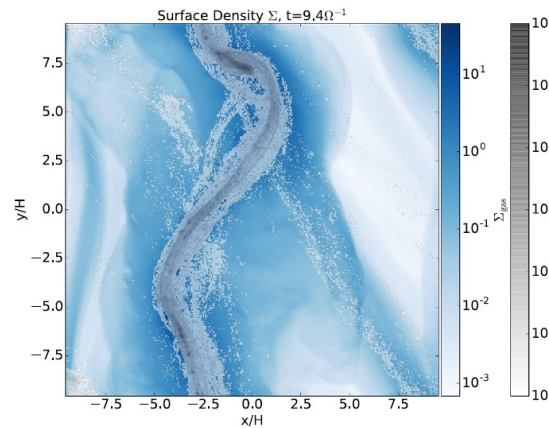
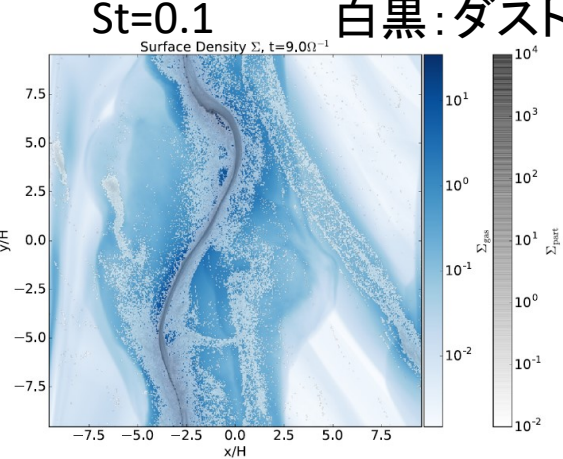
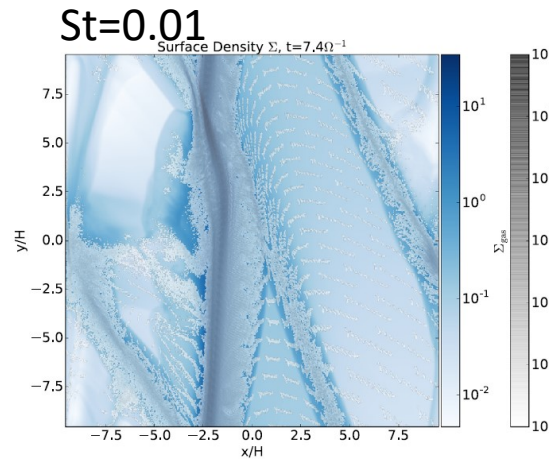
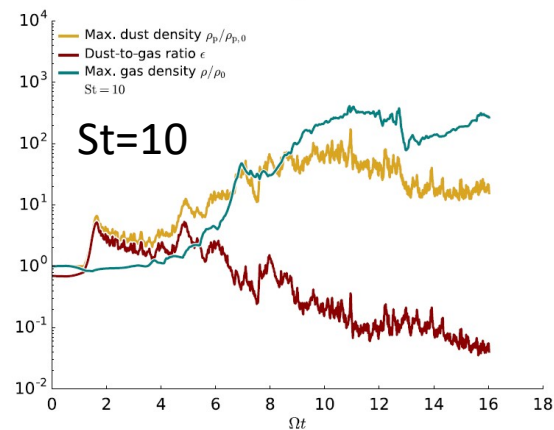
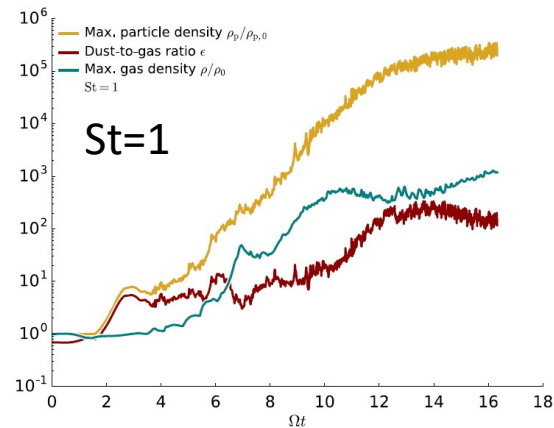
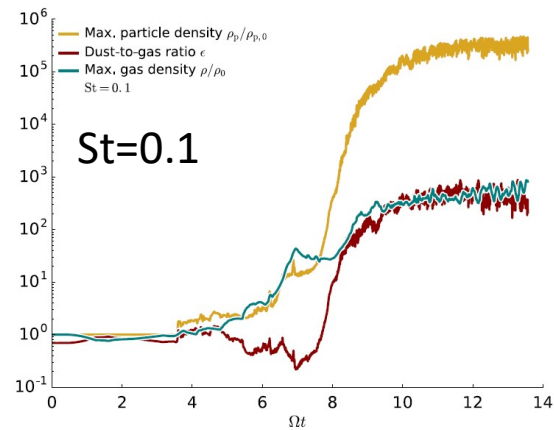
Max Planck Institute for Astronomy, Königstuhl 17, D-69117 Heidelberg, Germany; baehr@mpia.de

Received 2019 February 14; revised 2019 June 27; accepted 2019 July 2; published 2019 August 23

- 巨大惑星形成のシナリオ
 - Coreができた後でガスを纏う
 - 重力不安定性で作る
- ⇔ 木星の重力モーメントの観測により中心にコアがあることが示唆 (Bolton+2017)
- 目的
 - 重力不安定シナリオでもダストが集まってコアができるか？
 - Boley & Durisen (2010)で分裂片でダストが集積することを示しているが、より高解像度で調べる。
- 手法
 - 3次元shearing-box simulation using PENCIL code with $1024^2 \times 128$
 - β coolingを入れる。 $\Lambda \propto (T - T_0)t_c^{-1}$, $t_c = \beta\Omega^{-1}$
 - ダストはラグランジュ粒子として入れる(百万粒子)。
ダストーガス比は0.01。計算は単一サイズのダストでストークス数で指定

結果:コアの形成と大気の金属量

青:ガス
白黒:ダスト

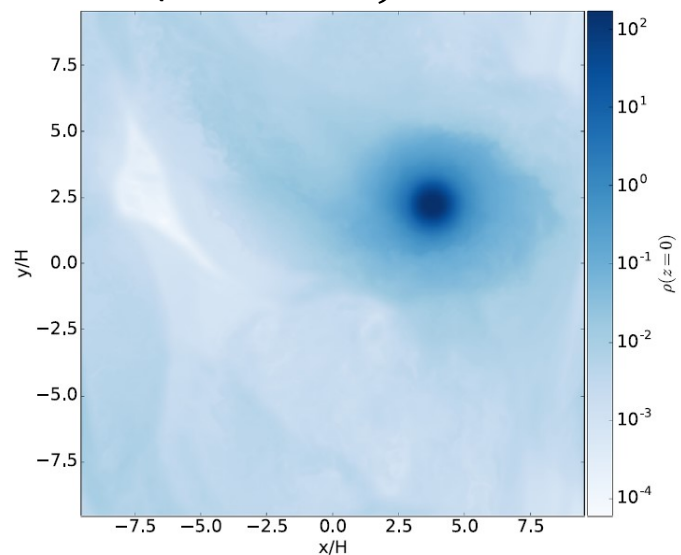


圧力極大にダストが集積

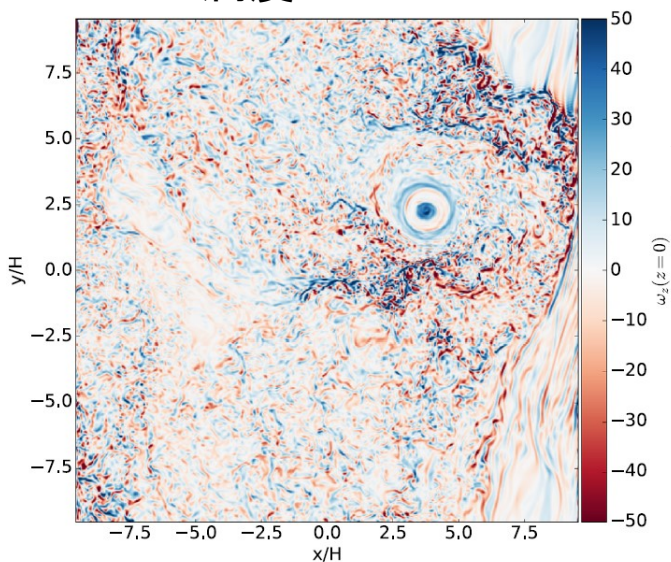
- St=0.01, 10のとき: 重力崩壊はしない
 - 大気の金属量は初期値より大きい
- St=0.1, 1のとき: 重力崩壊する
 - Several Jupiter masses with central solid cores typically of a few tens of M_{\oplus}
 - 大気の金属量は初期値より小さい

結果: satelliteの形成

ダストなし ($512^2 \times 64$)

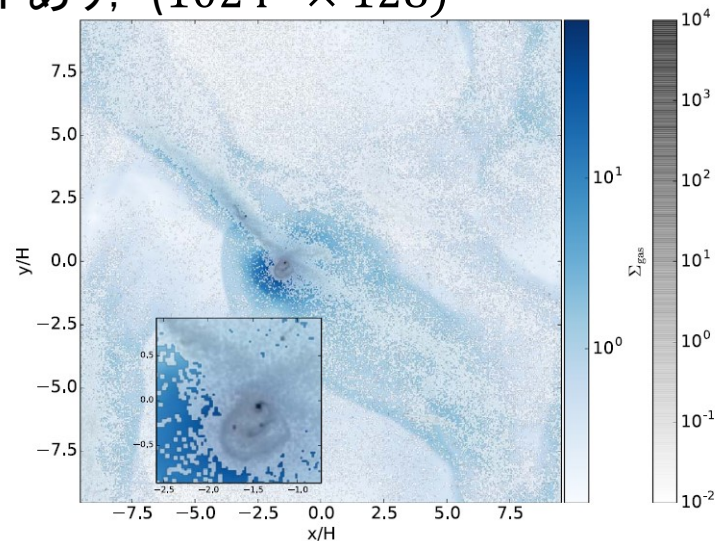


渦度

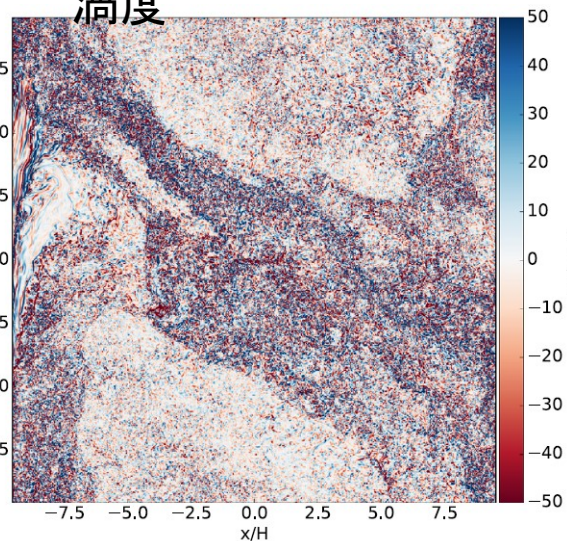


分裂片は
コヒーレントに回転

ダストあり, ($1024^2 \times 128$)



渦度



- 綺麗な回転は見られない。
- Coreの周囲に satellites ($\sim M_{\oplus}$) ができる。

The Transition from a Lognormal to a Power-law Column Density Distribution in Molecular Clouds: An Imprint of the Initial Magnetic Field and Turbulence

Sayantan Auddy¹, Shantanu Basu² and Takahiro Kudoh³

¹ Institute of Astronomy and Astrophysics, Academia Sinica, Taipei 10617, Taiwan; ² Department of Physics and Astronomy, The University of Western Ontario, London, ON N6A 3K7, Canada; ³ Faculty of Education, Nagasaki University, 1-14 Bunkyo-machi, Nagasaki 852-8521, Japan

E-mail contact: sauddy at asiaa.sinica.edu.tw

We introduce a theory for the development of a transitional column density Σ_{TP} between the lognormal and the power-law forms of the probability distribution function (PDF) in a molecular cloud. Our turbulent magnetohydrodynamic simulations show that the value of Σ_{TP} increases as the strength of both the initial magnetic field and turbulence increases. We develop an analytic expression for Σ_{TP} based on the interplay of turbulence, a (strong) magnetic field, and gravity. The transition value Σ_{TP} scales with \mathcal{M}_0^2 , the square of the initial sonic Mach number, and β_0 , the initial ratio of gas pressure to magnetic pressure. We fit the variation of Σ_{TP} among different model clouds as a function of $\mathcal{M}_0^2\beta_0$, or equivalently the square of the initial Alfvénic Mach number $\mathcal{M}_{\text{A}0}^2$. This implies that the transition value Σ_{TP} is an imprint of cloud initial conditions and is set by turbulent compression of a magnetic cloud. Physically, the value of Σ_{TP} denotes the boundary above which the mass-to-flux ratio becomes supercritical and gravity drives the evolution.

- 面密度頻度分布は低密度側はlog-normalで高密度側はpower lawになる
→ 臨界の面密度はどうやって決まっているのか？
- シミュレーション
 - 初期条件: 平板形状をしてsubcriticalな分子雲に乱流 (super Alfvénic) を与える。
- 圧縮されて密度が高くなったところで, 両極性拡散が効きsuper-criticalになる→重力収縮
 - $\tau_{\text{AD}} \propto L^2 \rho^{\frac{3}{2}} B^{-2} \propto \rho^{-0.5}$ ($L \propto \rho^{-0.5}, B \propto \Sigma \propto \rho H \propto \rho^{-0.5}$)
- 両極性拡散が効き始める面密度が臨界面密度になる。
- 計算により, 臨界面密度は乱流のAlfvén Mach numberに比例することがわかり, 解析的にも理解できる。

Probing the initial conditions of high-mass star formation

III. Fragmentation and triggered star formation

Chuan-Peng Zhang^{1,2,3}, Timea Csengeri³, Friedrich Wyrowski³, Guang-Xing Li^{4,5}, Thushara Pillai³, Karl M. Menten³, Jennifer Hatchell⁶, Mark A. Thompson⁷, and Michele R. Pestalozzi⁸

Context. Fragmentation and feedback are two important processes during the early phases of star formation.

Aims. Massive clumps tend to fragment into clusters of cores and condensations, some of which form high-mass stars. In this work, we study the structure of massive clumps at different scales, analyze the fragmentation process, and investigate the possibility that star formation is triggered by nearby H II regions.

Methods. We present a high angular resolution study of a sample of massive proto-cluster clumps G18.17, G18.21, G23.97N, G23.98, G23.44, G23.97S, G25.38, and G25.71. Combining infrared data at 4.5, 8.0, 24, and 70 μm , we use few-arcsecond resolution radio- and millimeter interferometric data taken at 1.3 cm, 3.5 mm, 1.3 mm, and 870 μm to study their fragmentation and evolution. Our sample is unique in the sense that all the clumps have neighboring H II regions. Taking advantage of that, we test triggered star formation using a novel method where we study the alignment of the centres of mass traced by dust emission at multiple scales.

Results. The eight massive clumps, identified based on single dish observations, have masses ranging from 228 to 2279 M_{\odot} within an effective radius of $R_{\text{eff}} \sim 0.5$ pc. We detect compact structures towards six out of the eight clumps. The brightest compact structures within infrared bright clumps are typically associated with embedded compact radio continuum sources. The smaller scale structures of $R_{\text{eff}} \sim 0.02$ pc observed within each clump are mostly gravitationally bound and massive enough to form at least a B3-B0 type star. Many condensations have masses larger than 8 M_{\odot} at small scale of $R_{\text{eff}} \sim 0.02$ pc. We find that the two lowest mass and lowest surface density infrared quiet clumps with $< 300 M_{\odot}$ do not host any compact sources, calling into question their ability to form high-mass stars. Although the clumps are mostly infrared quiet, the dynamical movements are active at clump scale (~ 1 pc).

Conclusions. We studied the spatial distribution of the gas conditions detected at different scales. For some sources we find hints of external triggering, whereas for others we find no significant pattern that indicates triggering is dynamically unimportant. This probably indicates that the different clumps go through different evolutionary paths. In this respect, studies with larger samples are highly desired.

- 大質量クランプを異なるスケールで観測し, 近くのHII領域からの誘発の可能性を探る。
 - 1.3cm, 3.5mm, 1.3mm, 870umのデータと4.5, 8.0, 24, 70um
- 誘発の兆候はあまりなかった。(8個のクランプのうち3つはそれっぽい様子が見える) → 大きなサンプルでの研究が必要

OH maser emission in the THOR survey of the northern Milky Way

H. Beuther¹, A. Walsh², Y. Wang¹, M. Rugel^{1,3}, J. Soler¹, H. Linz¹, R.S. Klessen⁴, L.D. Anderson^{5,10,11}, J.S. Urquhart⁶, S.C.O. Glover⁴, S.J. Billington⁶, J. Kainulainen^{7,1}, K.M. Menten³, N. Roy⁸, S.N. Longmore⁹ and F. Bigiel¹²

Context: OH masers trace diverse physical processes, from the expanding envelopes around evolved stars to star-forming regions or supernovae remnants. Providing a survey of the ground-state OH maser transitions in the northern hemisphere inner Milky Way facilitates the study of a broad range of scientific topics.

Aims: We want to identify the ground-state OH masers at ~ 18 cm wavelength in the area covered by “The HI/OH/Recombination line survey of the Milky Way (THOR)”. We will present a catalogue of all OH maser features and their possible associated environments.

Methods: The THOR survey covers longitude and latitude ranges of $14.3^\circ < l < 66.8^\circ$ and $b < \pm 1.25^\circ$. All OH ground state lines $^2\Pi_{3/2}(J=3/2)$ at 1612 (F=1-2), 1665 (F=1-1), 1667 (F=2-2) and 1720 MHz (F=2-1) have been observed, employing the Very Large Array (VLA) in its C configuration. The spatial resolution of the data varies between $12.5''$ and $19''$, the spectral resolution is 1.5 km s^{-1} , and the rms sensitivity of the data is $\sim 10 \text{ mJy beam}^{-1}$ per channel.

Results: We identify 1585 individual maser spots (corresponding to single spectral features) distributed over 807 maser sites (regions of size $\sim 10^3 - 10^4 \text{ AU}$). Based on different criteria from spectral profiles to literature comparison, we try to associate the maser sites with astrophysical source types. Approximately 51% of the sites exhibit the double-horned 1612 MHz spectra typically emitted from the expanding shells of evolved stars. The separations of the two main velocity features of the expanding shells typically vary between 22 and 38 km s^{-1} . In addition to this, at least 20% of the maser sites are associated with star-forming regions. While the largest fraction of 1720 MHz maser spots (21 out of 53) is associated with supernova remnants, a significant fraction of the 1720 MHz maser spots (17) are also associated with star-forming regions. We present comparisons to the thermal $^{13}\text{CO}(1-0)$ emission as well as to other surveys of class II CH_3OH and H_2O maser emission. The catalogue attempts to present associations to astrophysical sources where available, and the full catalogue is available in electronic form.

Conclusions: This OH maser catalogue presents a unique resource of stellar and interstellar masers in the northern hemisphere. It provides the basis for a diverse range of follow-up studies from envelopes around evolved stars to star-forming regions and Supernova remnants.

First detections of H₁₃CO⁺ and HC₁₅N in the disk around HD 97048: Evidence for a cold gas reservoir in the outer disk

Alice S. Booth¹, Catherine Walsh¹ and John D. Ilee¹

¹ University of Leeds, Leeds LS2 9JT, UK

E-mail contact: pyasb *at* leeds.ac.uk

Observations of different molecular lines in protoplanetary disks provide valuable information on the gas kinematics, as well as constraints on the radial density and temperature structure of the gas. With ALMA we have detected H₁₃CO⁺ (J=4-3) and HC₁₅N (J=4-3) in the HD 97048 protoplanetary disk for the first time. We compare these new detections to the ringed continuum mm-dust emission and the spatially resolved CO (J=3-2) and HCO⁺ (J=4-3) emission. The radial distributions of the H₁₃CO⁺ and HC₁₅N emission show hints of ringed sub-structure whereas, the optically thick tracers, CO and HCO⁺, do not. We calculate the HCO⁺/H₁₃CO⁺ intensity ratio across the disk and find that it is radially constant (within our uncertainties). We use a physio-chemical parametric disk structure of the HD 97048 disk with an analytical prescription for the HCO⁺ abundance distribution to generate synthetic observations of the HCO⁺ and H₁₃CO⁺ disk emission assuming LTE. The best by-eye fit models require radial variations in the HCO⁺/H₁₃CO⁺ abundance ratio and an overall enhancement in H₁₃CO⁺ relative to HCO⁺. This highlights the need to consider isotope selective chemistry and in particular low temperature carbon isotope exchange reactions. This also points to the presence of a reservoir of cold molecular gas in the outer disk (T < 10 K, R > 200 au). Chemical models are required to confirm that isotope-selective chemistry alone can explain the observations presented here. With these data, we cannot rule out that the known dust substructure in the HD 97048 disk is responsible for the observed trends in molecular line emission, and higher spatial resolution observations are required to fully explore the potential of optically thin tracers to probe planet-carved dust gaps. We also report non-detections of H₁₃CO⁺ and HC₁₅N in the HD 100546 protoplanetary disk.